Available online at www.sciencedirect.com
SCIENCE DIRECT
Catalysis Today 104 (2005) 120–125
CATALYSIS TODAY
www.elsevier.com/locate/cattod

Synthesis and oxygen transport characteristics of dense and porous cerium/gadolinium oxide materials Interest in membrane reactors

C. Guizard [a,1], A. Julbe [a,*], O. Robbe [b], S. Sarrade [b]

[a] *Institut Européen des Membranes, UMR 5635, CNRS/UM2/ENSCM, CC 47, Place Eugène Bataillon, 34095 Montpellier Cedex 05, France*
[b] *Laboratoire des Fluides Supercritiques et des Membranes, CEA VALRHO, DEN/DTE/SLP, BP 111, 26702 Pierrelatte Cedex, France*

Available online 7 April 2005

Abstract

Cerium/gadolinium oxide (CGO)-based ceramic ion conductive membranes (CICMs) have potential uses in catalytic membrane reactors (CMRs) and solid oxide fuel cells (SOFCs). A supercritical CO_2 aided sol–gel process allowed the synthesis of CGO materials with the composition $Ce_{0.9}Gd_{0.1}O_{1.95}$. The produced nanophase powders were non-agglomerated, with a controlled morphology, a high purity and a high specific surface area (>100 m^2/g). The CGO cubic crystalline phase has been obtained at temperatures <300 °C, lower than those of conventional solid state chemistry routes. With respect to ionic oxygen transport, a high conductivity at intermediate temperature (2×10^{-2} S cm^{-1} at 600 °C), almost equivalent in dense and porous samples, has been obtained on sintered materials prepared from these powders. In relation to their porosity characteristics, a modelling approach successfully explained the high ionic oxygen transport of some specific porous samples. Future directions for preparing porous conductive ceramics well adapted to CMR or SOFC applications can be anticipated from this model.

Keywords: Cerium/gadolinium oxide; Sol–gel process; Ceramic ion conducting membrane

1. Introduction

The use of ceria in catalysis has attracted considerable attention in recent years [1]. Specifically, cerium/gadolinium oxide has potential uses for catalytic combustion processes like soot removal from diesel engine exhaust [2], for steam reforming [3,4], and in redox and electrochemical reactions for SOFC applications [5,6]. In electrochemical applications where substantial ionic bulk conductivity is expected, ceria doped with gadolinium (CGO material), namely the composition $Ce_{0.9}Gd_{0.1}O_{1.95}$, has a wider ionic domain and a higher conductivity at low temperature than the other gadolinium based compositions [5]. An important parameter in conductive ceramics is the contribution of grain boundary resistances. The grain boundary resistance may occur due to the presence of an amorphous glassy phase due to impurities, microporosity or segregation of the dopant ions in the boundaries. Accordingly, the purity and the sintering capability of the initial powder as well as the sintering process (temperature and duration) have a determining effect on the grain boundary resistance of the resulting materials.

The aim of this study was the preparation and the ionic oxygen transport investigation of nanophase CGO-based ceramic conductive membranes (CICMs) with structural and textural characteristics specially designed for catalytic membrane reactors (CMRs) or electrochemical devices like solid oxide fuel cells (SOFCs). We used an innovative method in supercritical CO_2 for the synthesis of CGO powders with the composition $Ce_{0.9}Gd_{0.1}O_{1.95}$. The combination of the supercritical antisolvent (SAS) processing method [7] with the sol–gel process is a very promising synthesis route [8] for the production of very pure and crystalline CGO powders with a high sintering capability.

* Corresponding author. Tel.: +33 4 67 14 91 42; fax: +33 4 67 14 91 19.
E-mail address: julbe@iemm.univ-montp2.fr (A. Julbe).
[1] Present address: Laboratoire de Synthèse et Fonctionnalisation des Céramiques, FRE2770, CNRS/SAINT-GOBAIN CREE, 550 Avenue Alphonse Jauffret, 84306 Cavaillon Cedex, France.

0920-5861/$ – see front matter © 2005 Elsevier B.V. All rights reserved.
doi:10.1016/j.cattod.2005.03.046

Moreover, it renders possible the preparation of supported CGO layers on porous supports, directly in the supercritical phase. Conductivity measurements were carried out on dense and porous CGO materials prepared from these powders, in order to analyse the effect of the porosity on ionic oxygen transport. These results are discussed in the light of theoretical models describing ionic transport in porous oxygen conductive ceramic materials [9,10].

2. Experimental

The precursors, cerium acetate (99.9% from Aldrich) and gadolinium acetate (99.9% from Strem), were used as purchased. A 8 wt.% nitric acid (65% from Fluka) solution in 2-propanol (99% from Prolabo) was used as the co-solvent for the preparation of 0.02 M solutions of cerium and gadolinium precursors. The ratio gadolinium/cerium was 1–10 in order to get the composition $Ce_{0.9}Gd_{0.1}O_{1.95}$.

Synthesis of CGO powders was carried out in a 0.5 L batch reactor equipped with a heating mantle and a mechanical stirring device. Maximum operating pressure and temperature for this reactor were 35 MPa and 350 °C. For all experiments a predetermined quantity of precursor solution was introduced in the reactor at 50 °C; then CO_2 was pumped in the reactor up to intermediate pressures calculated in order to reach a final pressure of 30 MPa at synthesis temperatures of 150, 200 and 300 °C, respectively. For the preparation of supported porous layers, a macro-porous α-alumina multilayer support and the solution of precursors were introduced simultaneously in the reactor and treated under the same conditions than for powder synthesis. Structural and textural characteristics were obtained by X-ray diffraction and scanning electron microscopy. The total conductivity (ionic and electronic) of dense or porous CGO materials was measured by impedance spectroscopy on pellets (thickness 1 mm, diameter 10 mm) obtained by uniaxial pressing (5 MPa) of the powders, followed by sintering at 1100 and 1350 °C, respectively.

3. Results and discussion

3.1. Preparation of CGO powders and CICM materials

The supercritical CO_2 aided sol–gel process used for the synthesis of CGO powders and the preparation of supported CGO layers results from the combination of a chemical synthesis method close to the colloidal sol–gel route and a physical transformation method based on the supercritical antisolvent (SAS) particle formation process. First, cerium and gadolinium cations are hydrolysed by the nitric acid present in 2-propanol, leading to cations complexation by nitrate anions. Condensation of these cations is likely to occur by olation and oxolation depending on the acido-basic conditions in the solution, yielding nanometric condensed species. Then, the as formed sol is put in contact with CO_2 under supercritical conditions. The supercritical fluid dissolves in the co-solvent, causing a rapid expansion of the solution that promotes the nucleation and growth of particles from the condensed species. The formation of the cubic CGO crystalline structure (cf. Fig. 1) in the reactor at $T \leq 300$ °C results from the effect of both pressure and temperature. The characteristics of the produced powders are reported in Table 1. Different powder morphologies were obtained at 30 MPa and 150, 200 and 300 °C with a high specific surface area (>100 m^2/g) and a high sintering

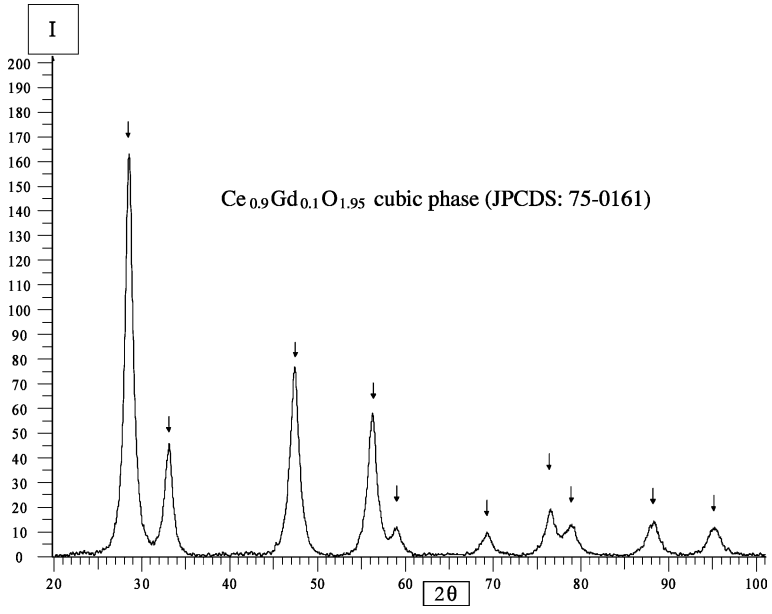

Fig. 1. X-ray diffraction pattern of a CGO powder prepared at 150 °C and 300 bar under supercritical conditions.

Table 1
Characteristics of crystalline CGO powders prepared by a supercritical CO_2 aided sol–gel process

Experimental conditions	Synthesis temperature (°C)	Crystallite size from XRD (nm)	Specific surface area (m^2/g)
Precursors (Ce and Gd acetates 0.16 M in isopropanol)	150	<5	139
Pressure (30 MPa)	200	<5	102
2-Propanol/CO_2 (80/20, v/v)	300	7	111

capability. An example of powder morphology for samples synthesized at 200 °C and the related dense structure obtained after sintering at 1350 °C are given in Fig. 2a and b, respectively.

A one step preparation procedure for supported CGO layers has been also successfully carried out by introducing both the α-alumina porous support and the CGO precursors solution in the reactor. The as prepared material, shown in Fig. 3, typically exhibits the asymmetric structure of a porous ceramic membrane. The CGO top-layer with a thickness <1 μm was deposited on the support at 150 °C, on the surface of its internal alumina layer (pore size 200 nm). However, CGO particles are also present in the support pores. This inert ceramic membrane support with a supported and/or infiltrated catalytically active material is of a great interest for membrane reactors working in a contactor mode [11]. The advantage of the supercritical CO_2 aided sol–gel method is the possibility of preparation at low temperature of porous conductive ceramic membranes or electrodes with a high specific surface area and therefore a high oxygen exchange capacity.

In order to study oxygen transport in these CGO membranes, porous and dense pellets were specially prepared for conductivity measurements. Samples were obtained by pressing the CGO powders in a mould followed by sintering respectively at 1100 and 1350 °C for obtaining porous and dense structures. The structure of the dense material (>96% d_{th}) is shown in Fig. 2b. Two porous structures obtained at 1100 °C from two different powders are shown in Fig. 4. One has an open and well connected 25% porosity with a 120 nm mean pore size (cf. Fig. 4a) whereas the second has a partially closed 26% porosity with a 150 nm mean pore size. Although the porous characteristics are almost the same for the two samples, the difference between the two porous structures clearly appears in the negative images shown in Fig. 4c and d. This difference has been attributed to the characteristics of the two powders used for sample preparation. In the following we have measured

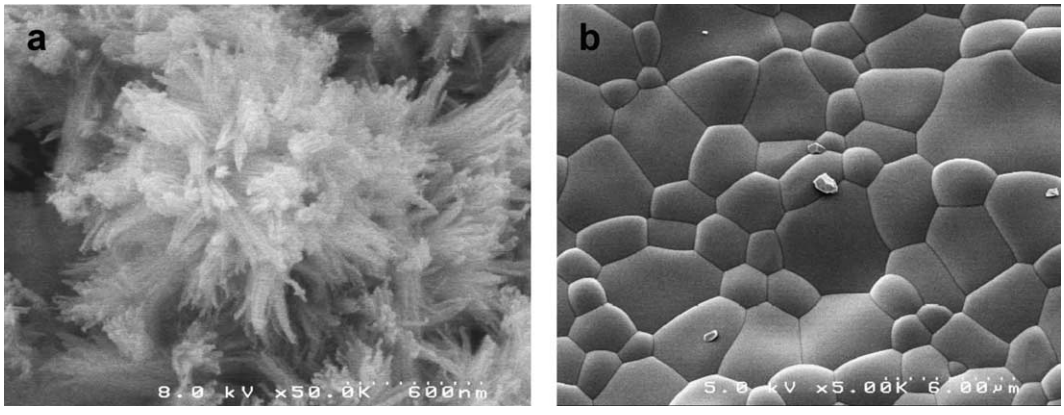

Fig. 2. Scanning electron microscopy images of a CGO powder (102 m^2/g) prepared at 200 °C (a), and of the corresponding dense material obtained after sintering at 1350 °C (b).

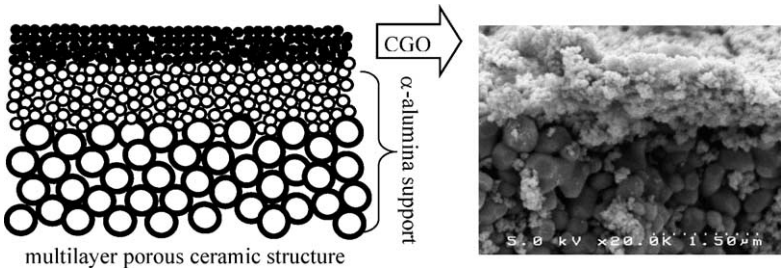

Fig. 3. Schematic representation of the porous asymmetric structure of the α-alumina ceramic support with the deposited CGO top-layer and the corresponding microscopy image.

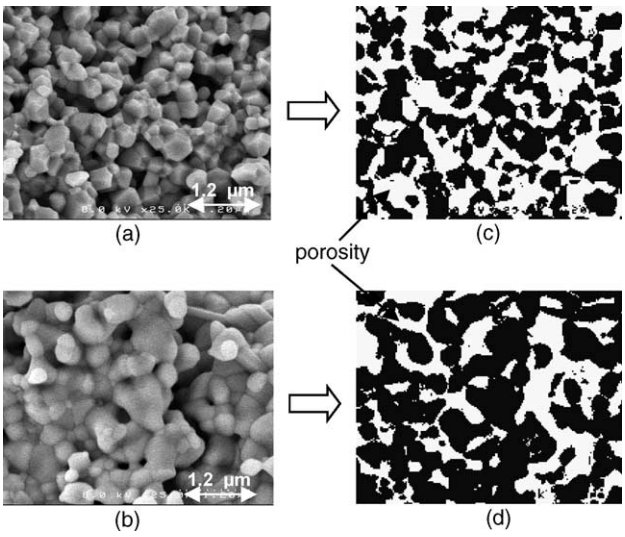

Fig. 4. Images of CGO sintered materials exhibiting a connected uniform porosity (a) and a non-uniform partially closed porosity (b). Corresponding negative images (c) and (d) showing porosity repartition in white and ceramic sintered grains in black, for the two samples.

the conductivity of these dense and porous CGO materials and tried to explain oxygen transport in relation with the porous structure.

3.2. Conduction properties and oxygen transport modelling

The measured total conductivity of the dense CGO material shown in Fig. 2b is among the highest conductivities at intermediate temperature (2×10^{-2} S cm^{-1} at 600 °C) published to date in the literature for this ceramic composition. This high level of conductivity has been attributed to the high purity of the CGO powders and to their high sintering capability yielding grain boundaries of very good quality. The activation energies E_a for total conductivity, $E_{a\text{-grain}}$ for intra-grain conductivity and $E_{a\text{-blocking}}$ for the blocking effect of grain boundaries are reported in Table 2. Interestingly, about the same values have been obtained for the sample shown in Fig. 4a with a uniform porosity. On the contrary, those calculated for the sample of Fig. 4b with a non-uniform porosity are notably higher. The difference in conductivity between these two materials has been attributed to their porous structure, which is connected for sample (a) and partially closed for sample (b).

Table 2
Activation energies related to measured conductivities in dense and porous CGO materials

CGO sample	Porosity	Grain size	E_a (eV)	$E_{a\text{-grain}}$ (eV)	$E_{a\text{-blocking}}$ (eV)
2b	Dense (4%)	>1 μm	0.75	0.62	0.81
4a	Open (25%)	250 nm	0.71	0.59	0.83
4b	Closed (26%)	190 nm	0.88	0.69	0.95

The role of connected porosity on conductivity can be better understood from theoretical models describing oxygen transfer in high temperature fuel cell porous electrodes which, by the way, can explain why an equivalent conductivity was found for the samples of Fig. 2b (dense) and Fig. 4a (porous). One of these models, proposed by Deng et al. [9,10], is of particular interest to predict the role of the porous structure in oxygen exchange and oxygen ion conductivity. In this model, a number of length scales are representative of the different phenomena involved in oxygen transport across a porous ion conductive ceramic medium. A prerequisite for this analysis is that the pore dimensions must be much smaller than the thickness L of the porous medium and the transport equations must be treated as being one-dimensional with the current flowing parallel to the direction of the pressure gradient.

Calculations are made starting from the length scale $L_d = D_{IE}/K$ (ratio of ion diffusion coefficient to surface reaction rate) that determines the transition from a diffusion limited transport, $L \gg L_d$, to a surface reaction limited transport, $L \ll L_d$. For the most common conductive ceramics at high temperature, L_d usually varies in a 50–100 μm range. The other length scales, L_p, L_g and L_m, account for gas diffusion in the pores and oxygen ion transport in the solid phase. They can be calculated from the porosity characteristics of the conductive ceramic in which $(1 - \phi)$ is the volume fraction of the solid; S is the pore wall surface area per unit volume, τ_s is the tortuosity of the solid phase and τ is the tortuosity of the porous structure. Other parameters involved in these calculations are the diffusion coefficients D_g and D_{IE} of the gas molecules and of the ambipolar pairs, and the concentrations c_i and c_g of the ions in the solid and of the gas molecules in the pores. Two cases are discussed hereafter in relation with the measured conductivities and the potential applications of the CGO materials studied in this work. One deals with a conductive material made of a virtual very thin non-porous layer in between two porous electrodes (discontinuous medium with no gas pressure variation in the pores on each side of the non-porous layer). The other concerns a homogeneous porous conductive material (gas pressure drop in a continuous porous medium). A schematic representation of the active regions for oxygen exchange in these porous media is shown in Fig. 5.

In the discontinuous medium, it is assumed that there is no gas pressure variation in the pores so that the entire pressure drop is across the non-porous layer. An active region defined by the length scale L_p (Eq. (1)) exists in the center of the material, on both sides of the virtual non-porous layer, where the gradient of the chemical potential of oxygen species between the gas phase in the pores and the solid phase in the ceramic grains allows enhanced ambipolar pairs transport in the solid. In other words, a substantial increase in ionic oxygen transport can be expected in SOFC porous electrodes exhibiting both a sufficient pore surface area and pore sizes large enough (submicronic pore sizes with a gas

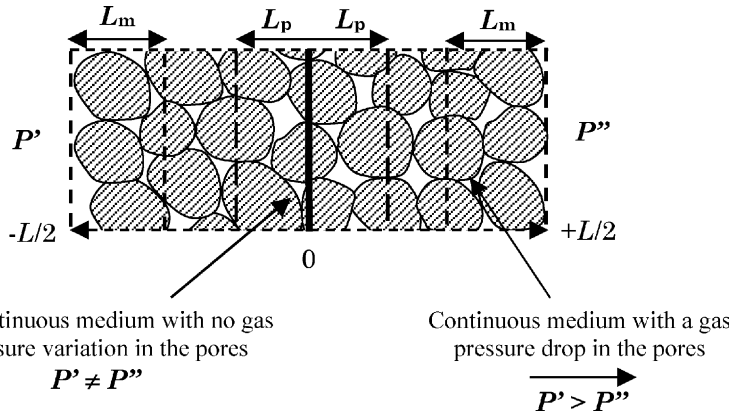

Fig. 5. Schematic representation of the cross section of a porous ion conducting ceramic material, showing the chemically active regions for oxygen exchange, defined by length scales L_p or L_m depending on porous characteristics, adapted from [9,10].

viscous flow mode) to prevent pressure variation in the pores:

$$L_p = \sqrt{\frac{L_d(1-\phi)}{S\tau_s}} \quad (1)$$

In the case where the porous material acts as a continuous medium, inducing a gas pressure drop in the pores, the oxygen molecules are considered to be consumed at the high pressure side and generated at the low pressure side. The length scale L_g (Eq. (1)) accounts for the variation in the chemical potential of the gas in the pores. This is typically the case for a mesoporous membrane in which gas flow obeys a Knudsen diffusion mechanism:

$$L_g = \sqrt{\frac{\tau_s \phi D_g c_g}{\tau(1-\phi) D_{IE} c_i}} L_p \quad (2)$$

In summary, as reported in Table 3, the model predicts that for a constant gas pressure in the pores, the chemically active regions for oxygen exchange are near the center of the porous material when $L_g > L_p$. This implies that for a thin electrolyte SOFC configuration, ionic current I in the electrodes can be theoretically enhanced for specific porous characteristics compared to the ionic current $I_{(s)}$ of the corresponding dense material. On the contrary for a membrane configuration, the chemically active regions L_m, calculated from Eq. (3), move out to outer interfaces of the membrane when $L_g \ll L_p$. Then the theoretical current enhancement $I/I_{(s)}$ is substantially reduced because of mass transport limitations (gas pressure drop in the pores). When $L_g \sim L_p$, the chemically active regions L_p and L_m are both at the center and at the outer boundaries of the porous material:

$$\frac{1}{L_m^2} = \frac{1}{L_g^2} + \frac{1}{L_p^2} \quad (3)$$

In the present case, the porous characteristics of the sample shown in Fig. 4a are close to those calculated in Table 3 for $S = 10^5\ cm^{-1}$ and d = 120 nm. In this case $L_g > L_p$ at $P = 1$ atm and $L_g \sim L_p$ at $P = 10^{-2}$ atm. The calculated values of L_p and L_m (~2 μm) are much smaller than the CGO pellet thickness (~1 mm) used for conductivity measurement. The 24- or 18-fold predicted current enhancements $I/I_{(s)}$ are in good agreement with the measured ionic oxygen transport for this sample. These results are very informative with regard to the required thickness and porosity characteristics of CICM in order to obtain a high ionic oxygen transport almost equal to the one obtained with the equivalent dense membrane. They show that our CGO materials are very promising for electrode or catalytic membrane applications.

4. Conclusion

The supercritical CO_2 aided sol–gel process allowed the preparation at low temperature (150 °C ≤ T ≤ 300 °C) of CGO crystalline powders with a high purity and a high

Table 3
Conductivity enhancement $I/I_{(s)}$ in a porous oxygen ion conductive ceramic material as a function of pore surface area S per unit volume and pore diameter d

S (cm^{-1})	d(nm)	L_p (μm)	P = 1 atm			$P = 10^{-2}$ atm			$P = 10^{-4}$ atm		
			L_g (μm)	L_m (μm)	$I/I_{(s)}$	L_g (μm)	L_m (μm)	$I/I_{(s)}$	L_g (μm)	L_m (μm)	$I/I_{(s)}$
10^6	12	0.77	3.3	0.75	72	0.34	0.31	29	0.034	0.034	4.4
10^5	120	2.4	24	2.4	24	3.4	2	18	0.34	0.34	4.2
10^4	1200	7.7	105	7.7	7.9	33	7.5	7.5	3.4	3.1	3.6

Calculation of length scales L_p, L_g and L_m assuming L_d = 100 μm and $D_{IE} = 5 \times 10^{-7}$ cm^2/s, from [10].

sintering capability. A partial or full densification of the CGO materials prepared from these powders can be easily achieved in the temperature range 1100–1350 °C. A one step process for the preparation of supported CGO porous layers in supercritical CO_2 has been also successfully demonstrated. Starting from powders with different characteristics, the influence of the porous structure on the ionic oxygen transport of sintered CGO materials has been clearly evidenced. Comparing two porous samples, one with a uniform and connected porosity, the other with a non-uniform and partially closed porosity led to the conclusion that the former has the best performance. In accordance with the prediction of the model, almost the same high conductivity (2×10^{-2} S cm^{-1} at 600 °C) has been obtained for the porous CGO material exhibiting a connected porosity and a sufficient pore surface area, compared to the corresponding fully dense material. These results show that it is possible to adapt, by the supercritical CO_2 aided sol–gel method, the textural characteristics of conductive ceramic materials to their expected applications: dense or porous membranes for oxygen distribution, or porous membranes and electrodes acting as catalytic contactors. Moreover, a modelling approach can be very helpful in anticipating new directions for the preparation of these specific porous or dense conductive ceramics. Work is underway for testing the catalytic efficiency of these CGO materials.

Acknowledgments

The authors would like to thank Mr. Fouletier, Mrs. Siebert and Mr. Dessemond from the LEPMI (UMR 5631 INPG-CNRS, University of Grenoble, France) for impedance spectroscopy measurements.

References

[1] A. Trovarelli, Catalysis by ceria and related materials, Imperial College Press, London, 2002.
[2] H. Christensen, Z.S. Rak, Catal. Today 75 (2002) 451.
[3] E. Ramirez-Cabrera, A. Atkinson, D. Chadwick, Appl. Catal. B: Environ. 47 (2004) 127.
[4] D-J. Liu, T.D. Kaun, H.-K. Liao, S. Ahmed, Int. J. Hydrogen Energy 29 (2004) 1035.
[5] B.C.H. Steele, Solid State Ionics 129 (2000) 95.
[6] B. Zhu, X.T. Yang, J. Xu, Z.G. Zhu, S.J. Ji, M.T. Sun, J.C. Sun, J. Power Sources 118 (2003) 47.
[7] R. Thiering, F. Dehghani, N.R. Foster, J. Supercrit. Fluids 21 (2001) 159.
[8] C. Guizard, A. Julbe, S. Sarrade, O. Robbe, S. Papet, in: Proceedings of the Eighth Meeting on Supercritical fluids, Bordeaux, France, 2002ISBN: 2-905267-34-8, p. 291.
[9] H. Deng, M. Zhou, B. Abeles, Solid State Ionics 74 (1994) 75.
[10] H. Deng, M. Zhou, B. Abeles, Solid State Ionics 80 (1995) 213.
[11] A. Julbe, D. Farrusseng, C. Guizard, J. Membr. Sci. 181 (2001) 3–20.